LOS ALAMOS SCIENTIFIC LABORATORY
of the
University of California
LOS ALAMOS • NEW MEXICO

Theoretical and Experimental Two-Dimensional Interactions of Shocks with Density Discontinuities

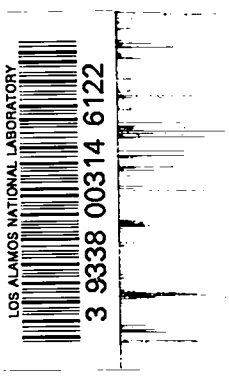

UNITED STATES
ATOMIC ENERGY COMMISSION
CONTRACT W-7405-ENG. 36

This report expresses the opinions of the author or authors and does not necessarily reflect the opinions or views of the Los Alamos Scientific Laboratory.

Printed in the United States of America. Available from
Clearinghouse for Federal Scientific and Technical Information
National Bureau of Standards, U. S. Department of Commerce
Springfield, Virginia 22151
Price: Printed Copy $3.00; Microfiche $0.65

LA-3614
UC-34, PHYSICS
TID-4500

LOS ALAMOS SCIENTIFIC LABORATORY
of the
University of California
LOS ALAMOS • NEW MEXICO

Report written: August 1966

Report distributed: February 10, 1967

Theoretical and Experimental Two-Dimensional Interactions of Shocks with Density Discontinuities

by

Charles L. Mader
Roger W. Taylor
Douglas Venable
James R. Travis

ABSTRACT

The "PHERMEX" radiographic facility has been used to study the interaction of shocks with cylindrical aluminum rods, "V" notches, and cylindrical voids in water. The experimental results are compared with two-dimensional numerical PIC (particle-in-cell) computations. Agreement between computation and experiment was within the resolution of the methods.

ACKNOWLEDGMENTS

The authors gratefully acknowledge the assistance and contributions of S. R. Orr and G. N. White, Jr., of T-5, F. H. Harlow of T-3, W. C. Davis of GMX-8, and R. K. London of GMX-11 of the Los Alamos Scientific Laboratory.

CONTENTS

		Page
	Abstract	3
	Acknowledgments	3
I.	Introduction	7
II.	Computational Method	7
III.	Experimental Method	7
IV.	Results	8
V.	Conclusions	11
	Literature Cited	11
	Figures	12

I. INTRODUCTION

The interaction of a shock wave with a cylindrical aluminum rod, a "V" notch, and a cylindrical void in water has been studied experimentally using the "PHERMEX"(1) radiographic facility of GMX-11. The cylindrical void has also been studied using the framing cameras of GMX-8. These systems were further studied numerically using the PIC technique for solving the two-dimensional hydrodynamics. Although the resolution available to the PIC technique from present computers is not detailed enough for many purposes, this is the only method available to describe the fluid flow of greatly distorted multicomponent systems. Therefore the experimental results should be useful in evaluating future numerical hydrodynamic schemes for treating similar complex flow problems.

II. COMPUTATIONAL METHOD

The particle-in-cell method for solving two-dimensional hydrodynamic problems has been described by its originator, F. H. Harlow of T-3, and his co-workers.(2) The particular version of his method that we used has been described by Mader.(3,4,5)

The explosive-Plexiglas driving system was approximated as a constant-velocity piston whose velocity was adjusted to give the experimentally observed unperturbed position of the shock as it interacted with the density discontinuity. The equation of state parameters for water and aluminum were identical to those described in reference 6. The cell size was 0.078125 cm for the cylindrical void and aluminum rod computations and 0.03125 cm for the "V" notch computations. The resolution of the computations was, at best, $\pm$ 0.05 cm.

III. EXPERIMENTAL METHOD

The "PHERMEX"(1) radiographic facility was used by Taylor and Venable to study the interaction of a shock with the density discontinuities in water. A sketch of the experimental setup is shown in Fig. 1.

The shocks were generated by a 4 x 4 x 8-in.-long block of Composition B initiated by a P 40 plane-wave lens. The water was contained in a 4 x 4-in. Plexiglas box with 1/4-in.-thick sides and bottom and 1/16-in.-thick front and back walls, placed on top of the pad of explosive. The density discontinuities were aligned in the box so that the axis of the radiographic beam was identical with the longitudinal axis of the discontinuity. This arrangement permitted maximum radiographic resolution which was approximately ± 0.1 μsec and ± 0.02 cm without time smear or ± 0.05 cm with time smear for a 0.5-cm/μsec shock velocity.

The x-ray pulse was produced by a burst of 20-MeV electrons impinging upon a 3-mm-diameter tungsten target resulting in radiation intensities up to 0.4 roentgen at the Plexiglas box, which was positioned approximately 3 meters from the target. The x-ray film was placed approximately 0.75 meters behind the box in a protective aluminum case.

The shock wave was plane for purposes of comparison with the computed model. Figure 7 shows the results of shots using an 8 x 8 x 8-in. pad of explosive to obtain a more nearly plane shock wave. The interactions with a cylindrical void of shocks produced by the 8 x 8-in. and the 4 x 4-in. driver were essentially the same. We conclude that the curvature of the wave does not have an important effect on the results.

The experimental shock wave was not flat-topped, and became attenuated as it ran through the water. The following measurements of the shock velocity of the front were made using pins.

Distance from Plexiglas-Water Interface to Shock Front (cm)	Time (μsec)	Average Incremental Shock Velocity (cm/μsec)	Average Pressure (kbars)
1.985	3.20	0.62	184
2.993	4.90	0.59	161
3.995	6.72	0.55	135

IV. RESULTS

The experimentally observed interaction of a shock with an aluminum rod in water is well described by the computations as is shown in Table I and in Figs. 2 and 3.

The experimentally observed interaction of a shock with a "V" notch in water also appears to be well described by the computations as is shown in Table II and in Figs. 4 and 5. Density variations observed in the jet region are qualitatively reproduced by the computations; however, a quantitative comparison is not possible because of the lack of detail of the computations. It is interesting to note the large differences between the radiographs of a shock interacting with a "V" notch in water and those of a shock interacting with a "V" notch in aluminum.(1) The

Table I. Comparison of Experimental Results and Computations of the Interaction of a Shock with a 1-cm-Radius Aluminum Rod in Water

	Time after Shock Arrived at Plexiglas-Water Interface							
	4.9 μsec		6.0 μsec		8.1 μsec		9.5 μsec	
	Exp.	Comp.	Exp.	Comp.	Exp.	Comp.	Exp.	Comp.
Axial thickness (height) of Al rod (cm)	1.89	1.88	1.67	1.69	1.70	1.70	1.60	1.55
Radial thickness (width) of Al rod (cm)	2.00	2.00	2.10	2.05	2.20	2.20	2.30	2.25
Axial distance of shock wave above top of Al rod (cm)	-	-	-	-	0.45	0.45	0.70	0.75
Maximum radial distance of reflected shock wave from axis of Al rod (cm)	1.20	1.23	1.90	1.80	3.20	3.30	3.90	3.80

Table II. Comparison of Experimental Results and Computations of the Interaction of a Shock with a "V" Notch in Water

	Time After Shock Arrived at Apex of "V" Notch			
	1.5 μsec		2.5 μsec	
	Exp.	Comp.	Exp.	Comp.
Distance of jet peak above initial apex of "V" notch (cm)	0.90	0.89	1.45	1.47
Distance of lowest part of jet above initial apex of "V" notch (cm)	0.70	0.72	1.10	1.12

Table III. Comparison of Experimental Results and Computations of the Interaction of a Shock with a Cylindrical Void in Water

	Time After Shock Arrived at Plexiglas-Water Interface					
	4.9 μsec		5.9 μsec		7.6 μsec	
	Exp.	Comp.	Exp.	Comp.	Exp.	Comp.
Distance of jet at axis above initial bottom of void (cm)	0.70	0.69	1.30	1.31	2.40	2.50

"V" notch in aluminum shows greater density gradients because of complicated spalling and elastic behavior of the aluminum. A fluid computation such as that used in this report, since it does not include spalling or elastic effects, yields similar results for water and aluminum "V" notches. While the computations appear to reproduce the water "V" notch radiographic results, they are completely inadequate to describe the aluminum "V" notch.

Finally, the experimentally observed interactions of a shock with a cylindrical void both in water and in polyethylene are shown in Figs. 6 and 7. The computed interaction of a shock with a cylindrical void in water is shown in Fig. 8. The experimental radiographs and the computations agree well except near the time of closure of the void. The agreement is good both when the void is approximately half-closed and after the shock has traveled about half of the void diameter above the top of the void. Between these positions the computations correctly predict the

position of the jet at the axis, as shown in Table III, but the water appears to move faster than was predicted above the equator of the void between the outer rim and the axis. Additional evidence of the position of this region is shown in Fig. 9. Framing camera pictures of the closure of a 1-cm-radius void in polyethylene with a shot geometry identical to that of the PHERMEX shots were taken by J. Travis and W. Morton. Figure 10 shows the void profile from the computations, the framing camera, and PHERMEX, when the hole is approximately 5/6 closed at the axis. The difference between the PHERMEX and framing camera pictures is probably caused by the low density region between the outer rim of the void and the high density region at the axis; the framing camera positions are not density-dependent as are the PHERMEX results. The computations closely reproduce the density gradients of the PHERMEX radiograph. The computations and framing camera pictures agree well except that the outer rim is closing faster in the computations. This difference is within the resolution of the computations and of the shock curvature and attenuation effects present in the experimental results.

V. CONCLUSIONS

Agreement between the dynamic radiographs and the numerical PIC computations of the interaction of a shock with an aluminum rod and with a "V" notch in water was obtained within the error of approximately $\pm$ 0.05 cm or $\pm$ 5% of the initial density discontinuity radius or height in the experimental and numerical resolution of the interfaces and shock positions. The radiographs and the computations of the interaction of a shock with a cylindrical void in water agree well except near the time of closure of the void. The agreement between the framing camera pictures and the computations is satisfactory.

The experimental results should be useful for evaluating future numerical hydrodynamic schemes.

LITERATURE CITED

1. Venable, D., "PHERMEX," Physics Today 17, No. 12, p. 19 (1964).
2. Harlow, F. H., "The Particle-in-Cell Computing Method for Fluid Dynamics," in Methods in Computational Physics, Alder, Fernbach, and Rotenberg, Eds. (Academic Press, New York, 1964), Vol. 3, pp. 319-343. Amsden, A. A., "The Particle-in-Cell Method for the Calculation of the Dynamics of Compressible Fluids," Los Alamos Scientific Laboratory Report LA-3466, 1966.
3. Mader, Charles L., "The Two-Dimensional Hydrodynamic Hot Spot," Los Alamos Scientific Laboratory Report LA-3077, 1964.

4. Mader, Charles L., "The Two-Dimensional Hydrodynamic Hot Spot, Vol. II," Los Alamos Scientific Laboratory Report LA-3235, 1964.

5. Mader, Charles L., "Initiation of Detonation by the Interaction of Shocks with Density Discontinuities," Phys. Fluids 8, 1811 (1965).

6. Mader, Charles L., "The Two-Dimensional Hydrodynamic Hot Spot, Vol. III," Los Alamos Scientific Laboratory Report LA-3450, 1966.

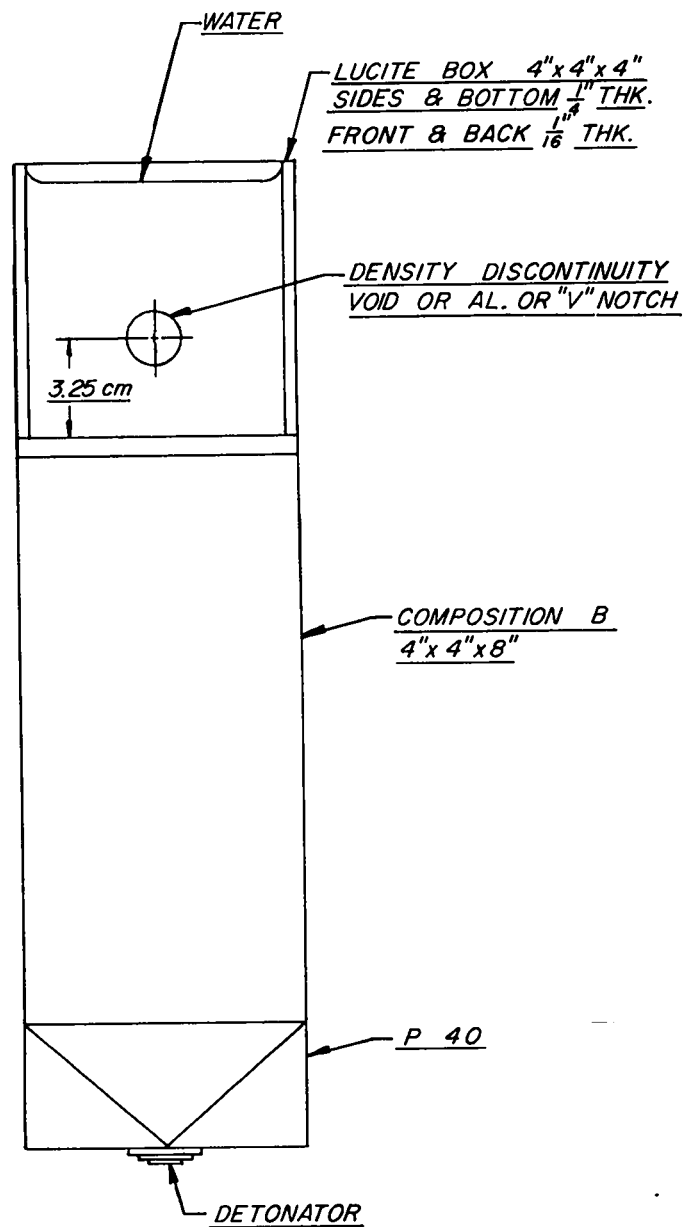

Fig. 1. The experimental assembly

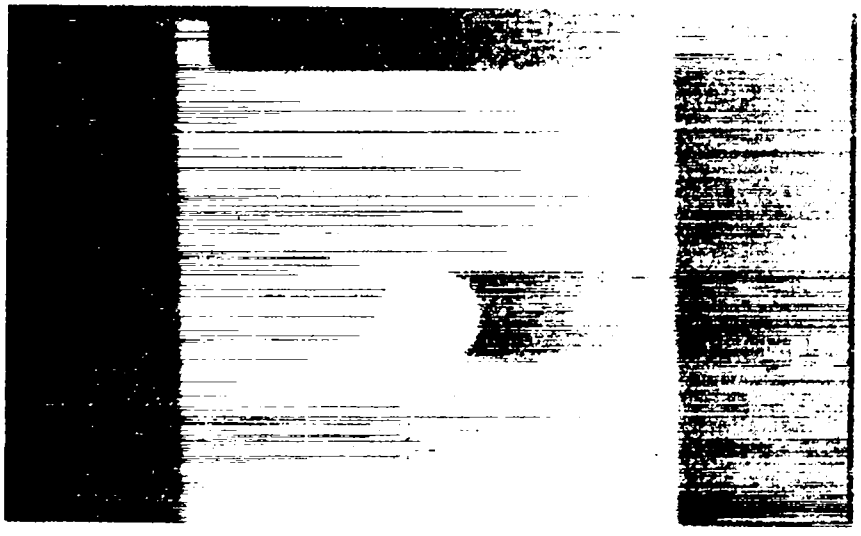

Initial geometry

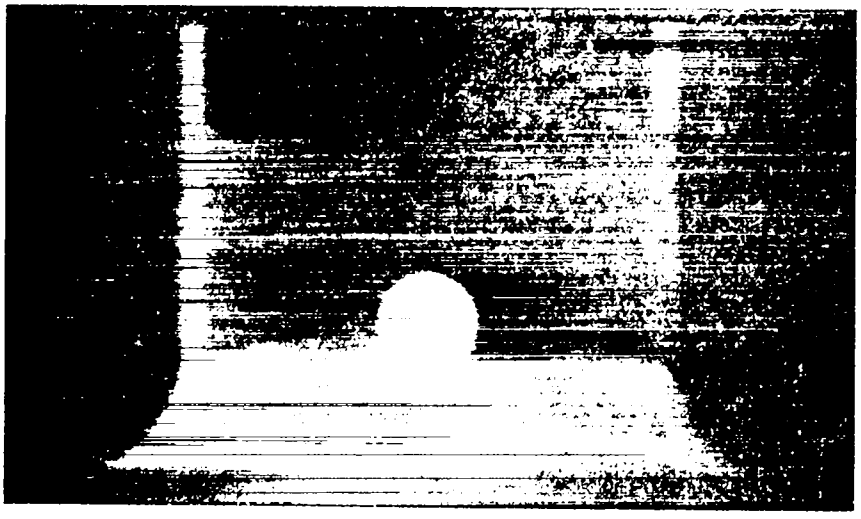

4.9 μsec

Fig. 2. PHERMEX radiographs of a 1-cm-radius aluminum rod in water centered 3.25 cm above the inside bottom of a Plexiglas box at various times after the shock arrived at the Plexiglas-water interface. The multiple image at the bottom of the rod is a result of the rod's being less compressed at the surface of the box than at the interior.

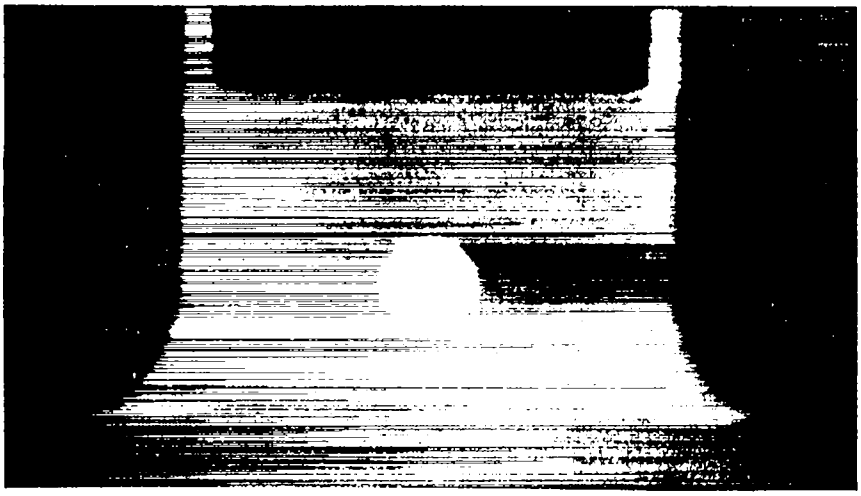

6.0 μsec

8.1 μsec

9.5 μsec

Fig. 2 (continued)

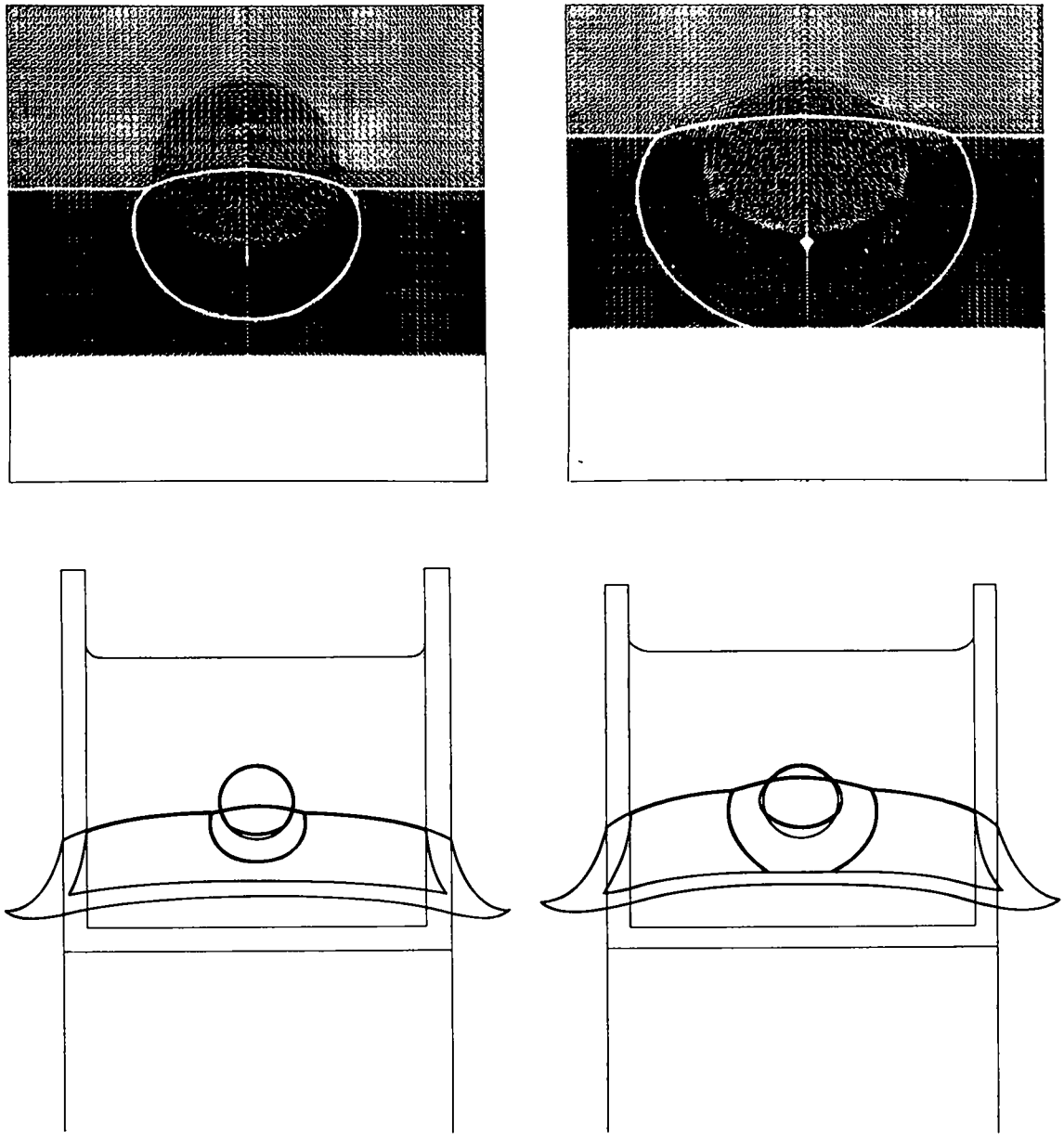

4.9 μsec 6.0 μsec

Fig. 3. The computed interaction of a shock with a 1-cm-radius aluminum rod in water. The rod is centered 3.25 cm above the piston. The times are after the shock arrival at the Plexiglas-water interface. A constant-pressure, 155-kbar piston is assumed. On the first page, the computed shock profile, and on the second page, the computed rod profile, are drawn on the computed results. Sketches of the prominent features from the radiographs are also provided.

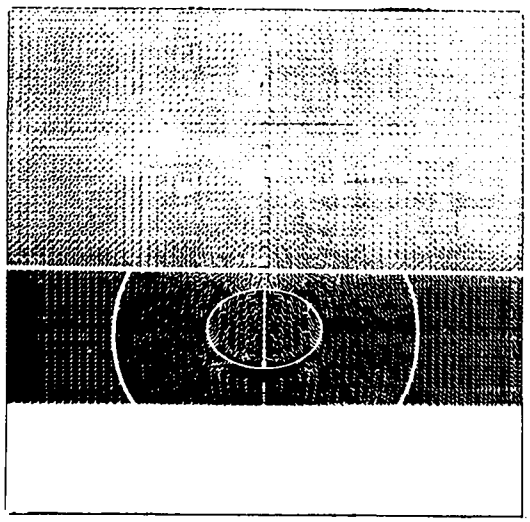

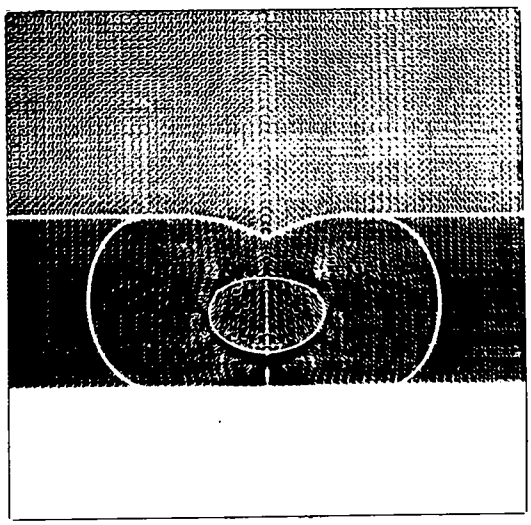

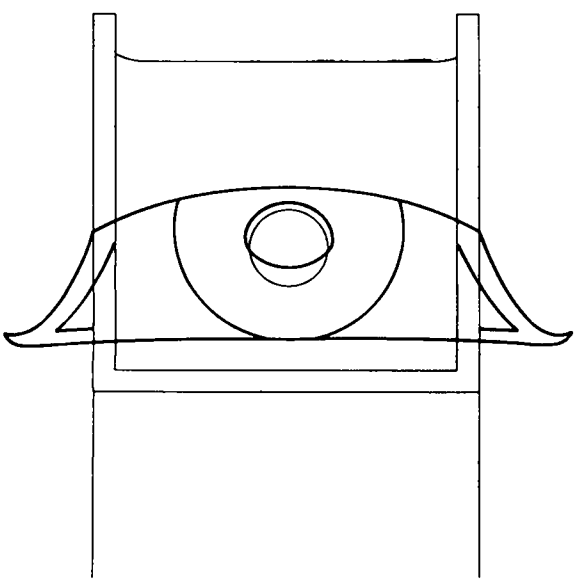

8.1 μsec

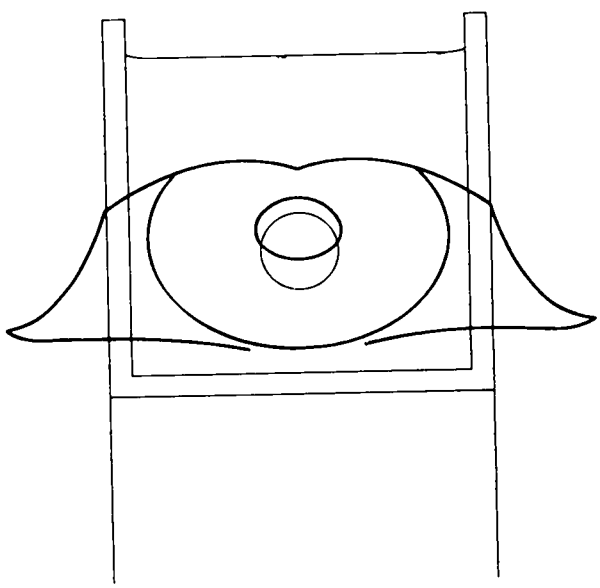

9.5 μsec

Fig. 3 (continued)

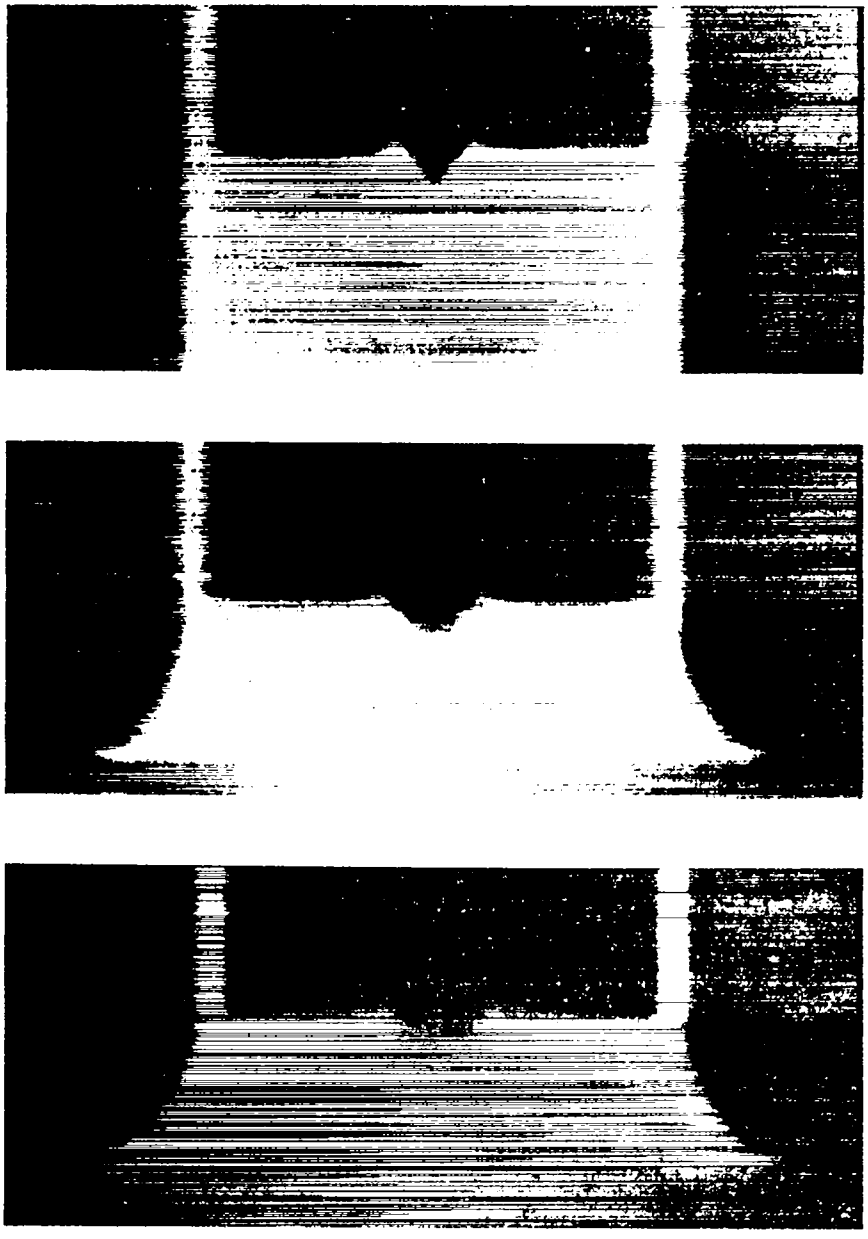

Fig. 4. PHERMEX radiographs of a 0.9-cm-deep "V" notch in water whose apex is 3.25 cm above the inside bottom of a Plexiglas box. The first shows the initial geometry of the shots; the next two were made 1.5 and 2.5 μsec after the shock arrived at the apex of the "V" notch, or 5.8 and 6.8 μsec after it arrived at the Plexiglas-water interface. The "V" notch was formed by thin (0.004-in.) plastic sheets.

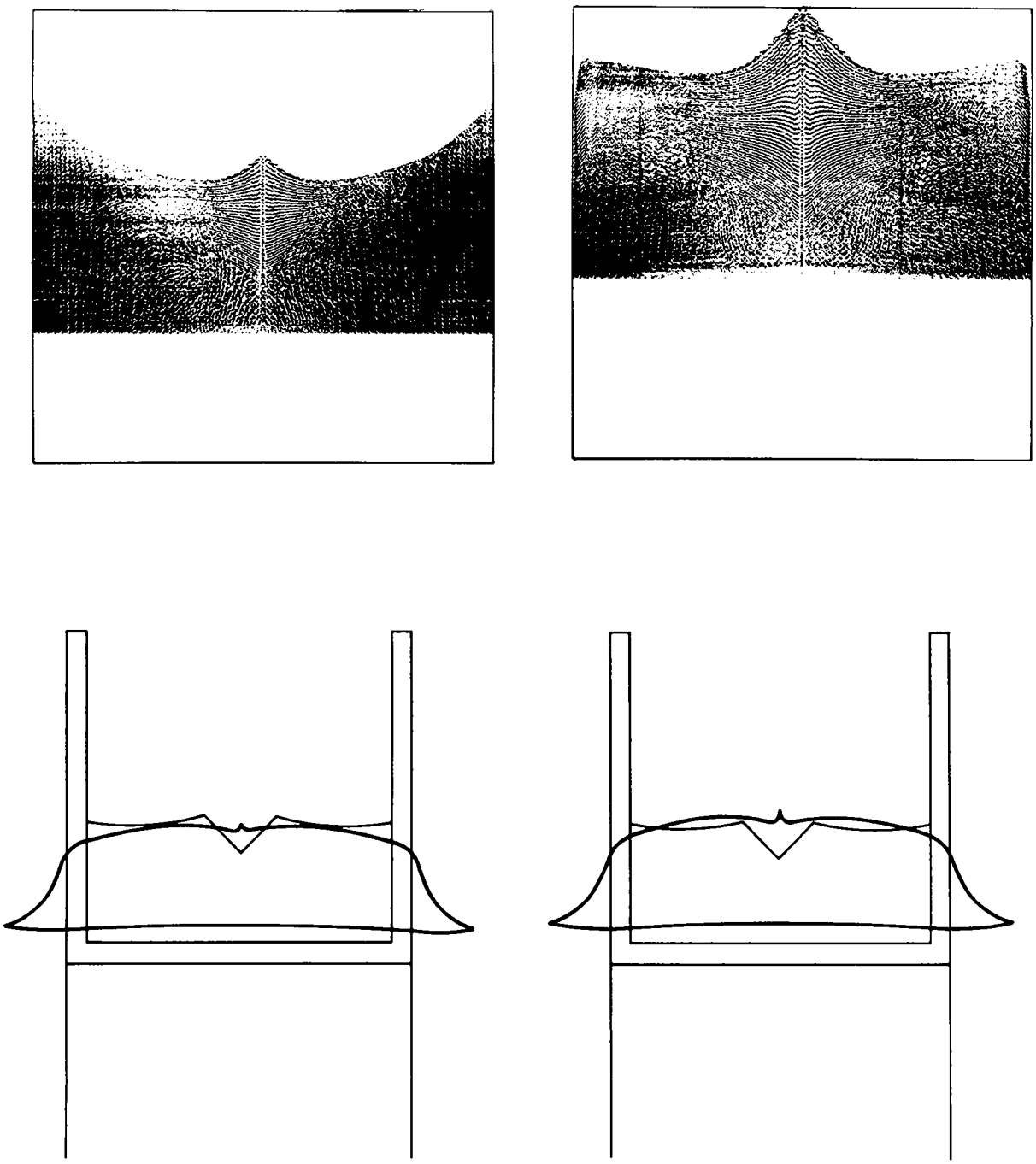

Fig. 5. The computed interaction of a shock in water with a 1-cm-deep "V" notch whose apex is 0.5 cm above the piston. A constant-pressure, 121-kbar piston was used. Sketches of the prominent features of radiographs made at the same times after the shock reacted with the apex are provided. The computations describe the center two square centimeters of the area shown by the radiographs.

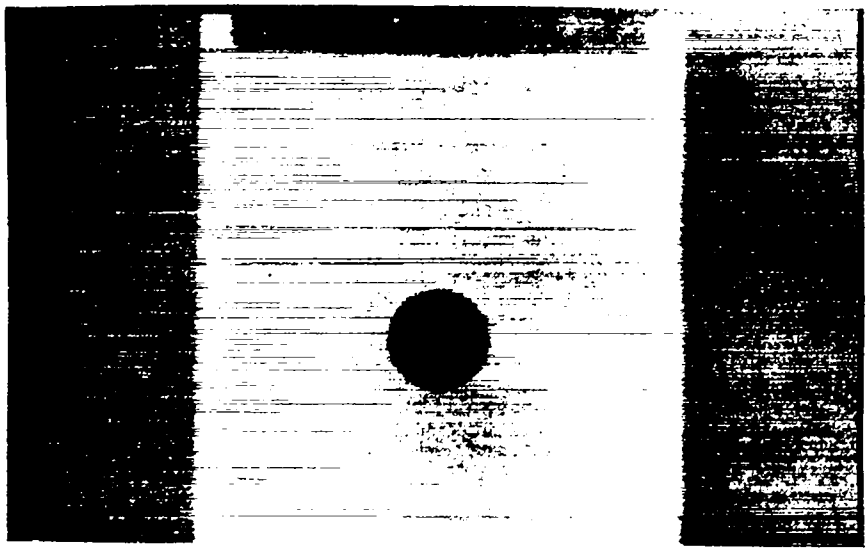

Initial geometry

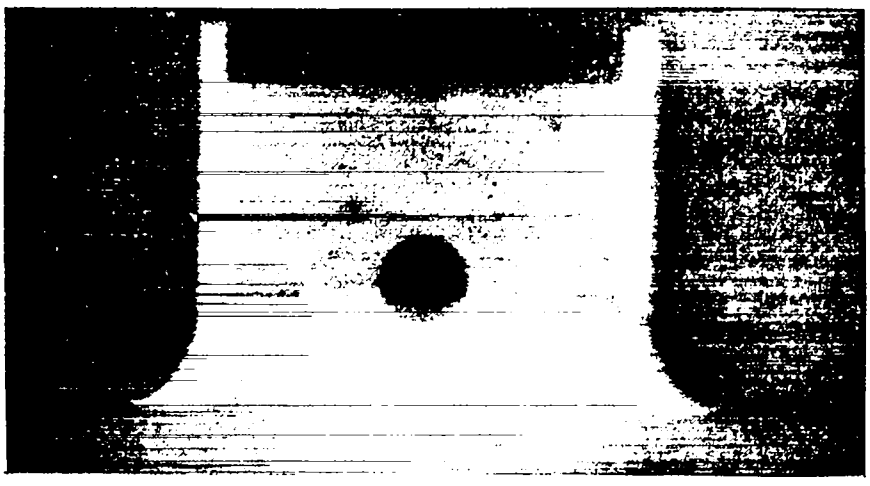

4.9 μsec

Fig. 6. PHERMEX radiographs of a 1-cm-radius cylindrical void in water centered 3.25 cm above the inside bottom of a Plexiglas box at various times after the shock arrived at the Plexiglas-water interface. The sixth and seventh frames are identical to the first and third, respectively, except that the cross sections of the box and explosive driving system are twice as large. These show that the wave curvature has a negligible effect on the results. The cylindrical void was formed by a thin-walled (0.006-in.) glass tube.

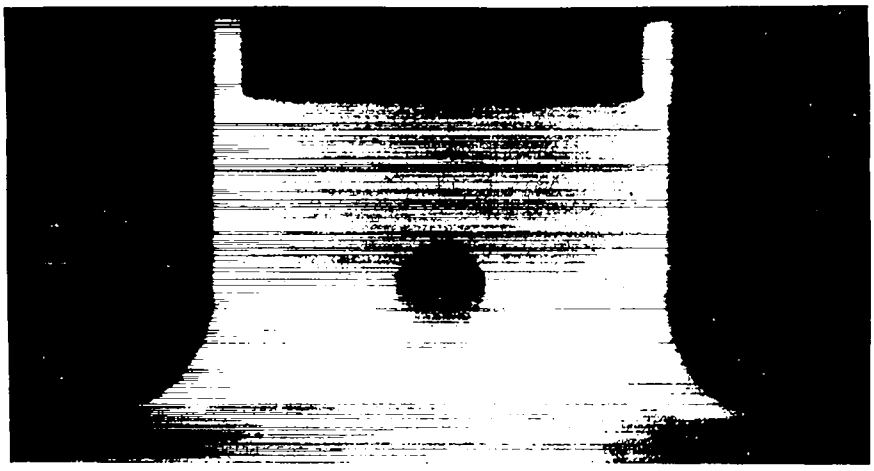

5.9 μsec

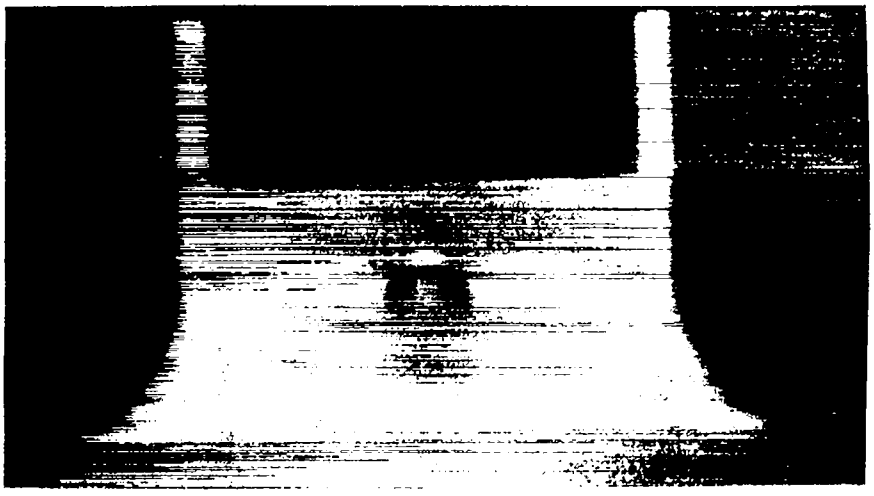

7.6 μsec

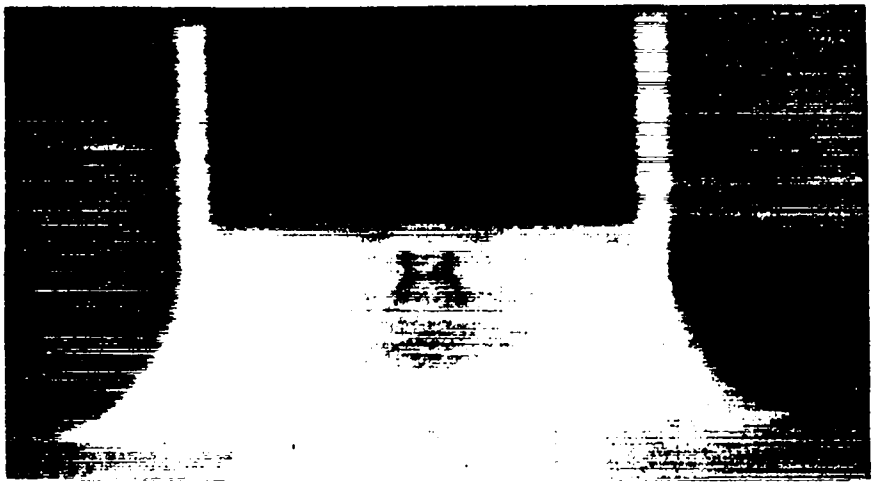

9.0 μsec

Fig. 6 (continued)

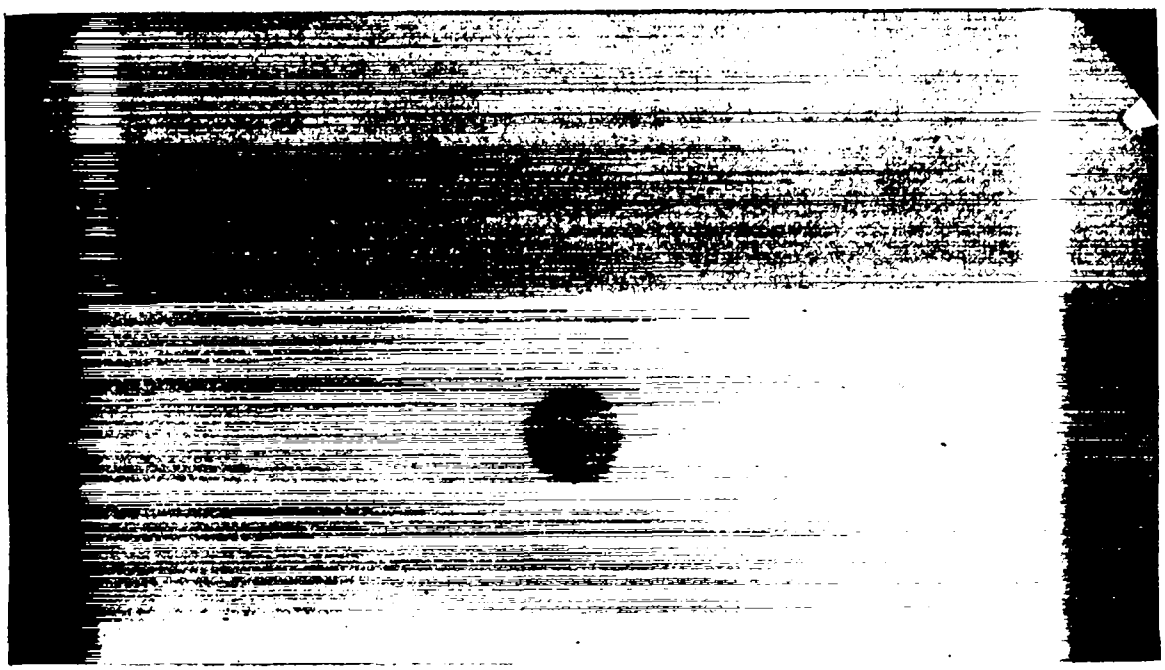

Initial geometry

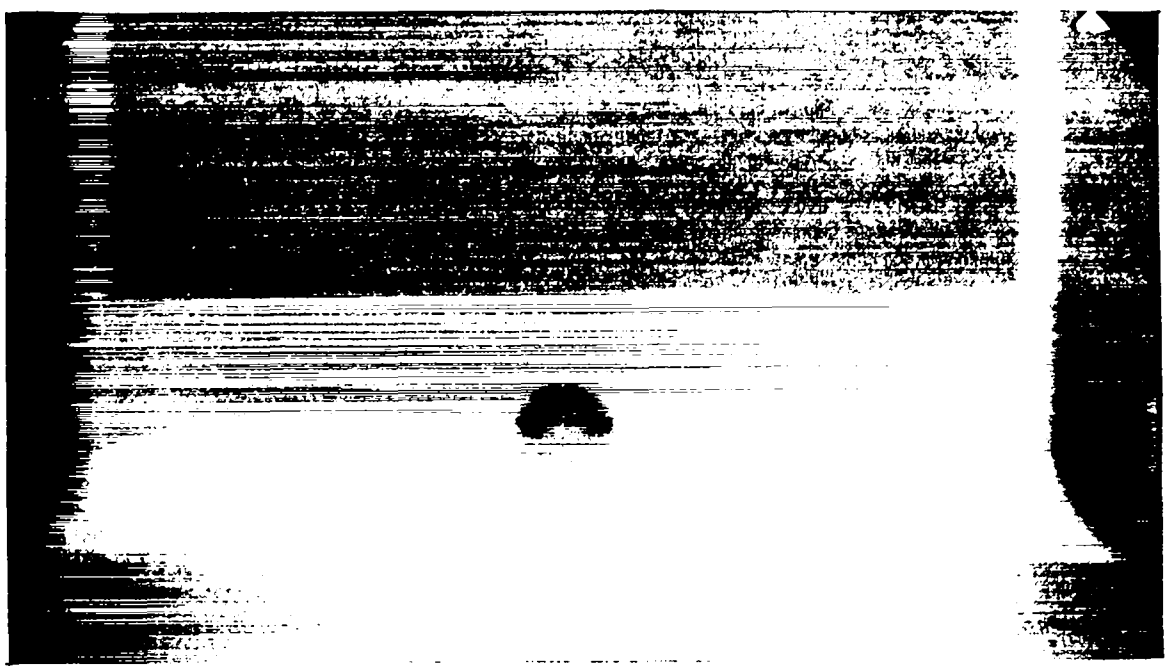

5.9 μsec

Fig. 6 (continued)

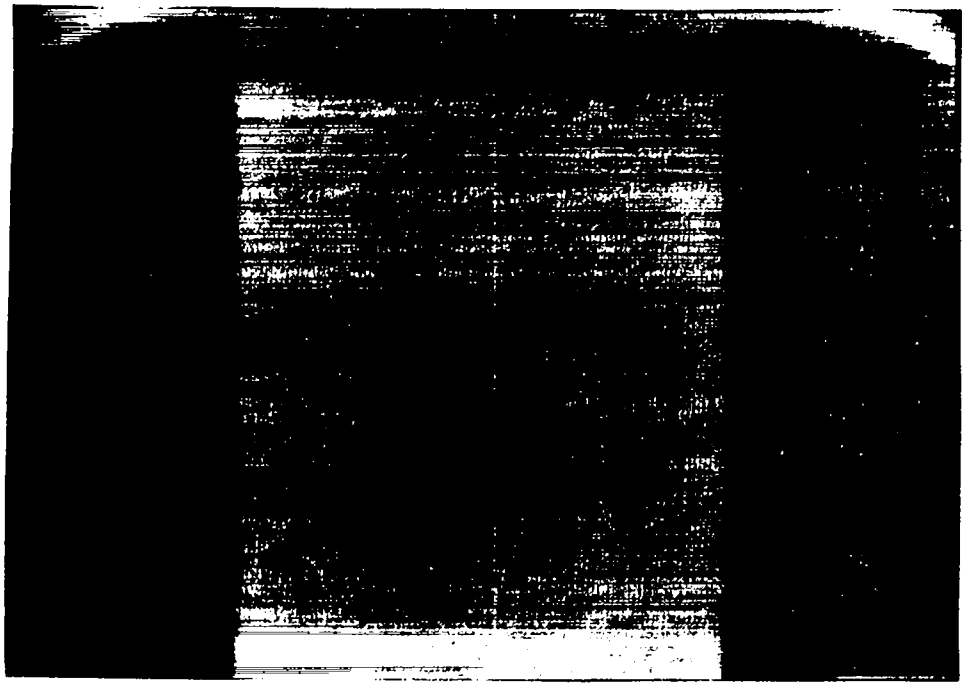

Initial geometry

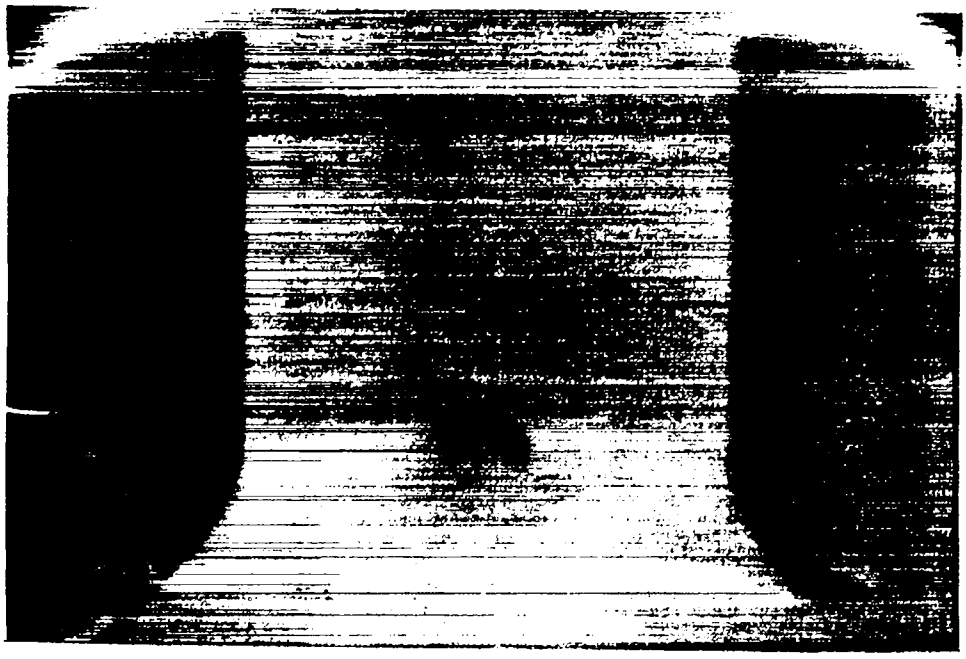

6.2 μsec

Fig. 7. PHERMEX radiographs of a 1-cm-radius void in polyethylene in the same geometry as Fig. 6, at various times after the shock arrived at the Plexiglas-polyethylene interface. The void in the first shot was evacuated to less than 0.05 mm of mercury to show that the effect of air is negligible.

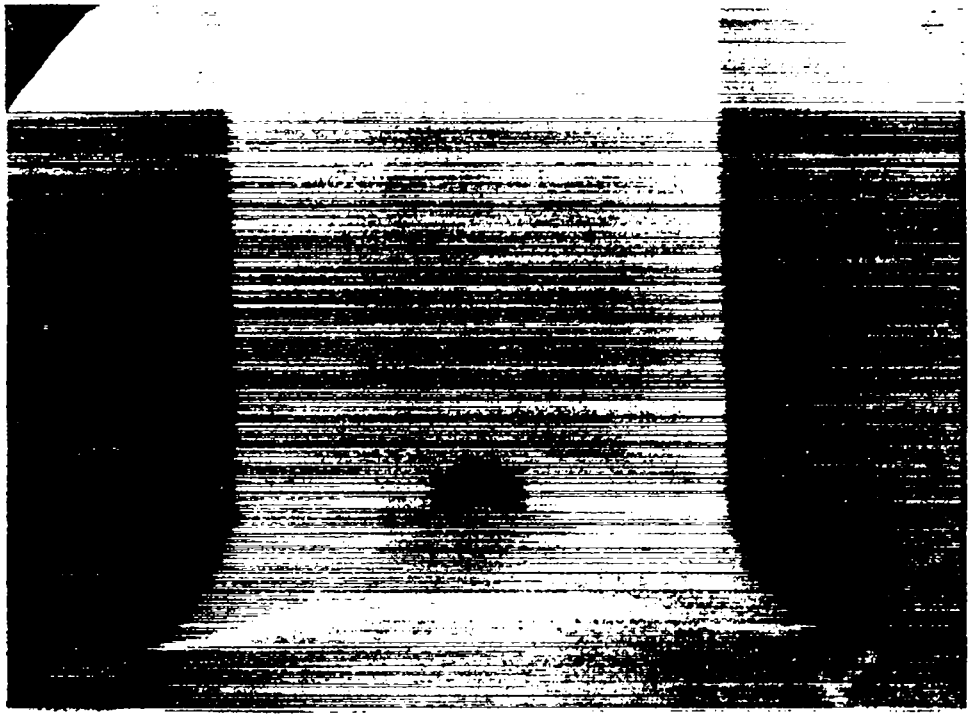

6.3 μsec

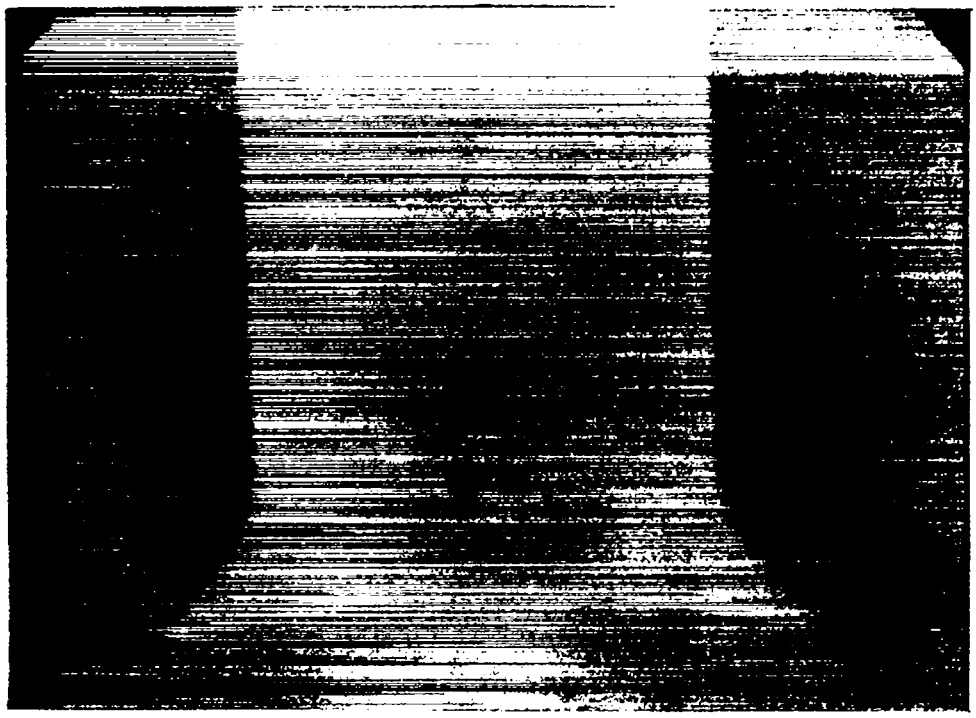

7.7 μsec

Fig. 7 (continued)

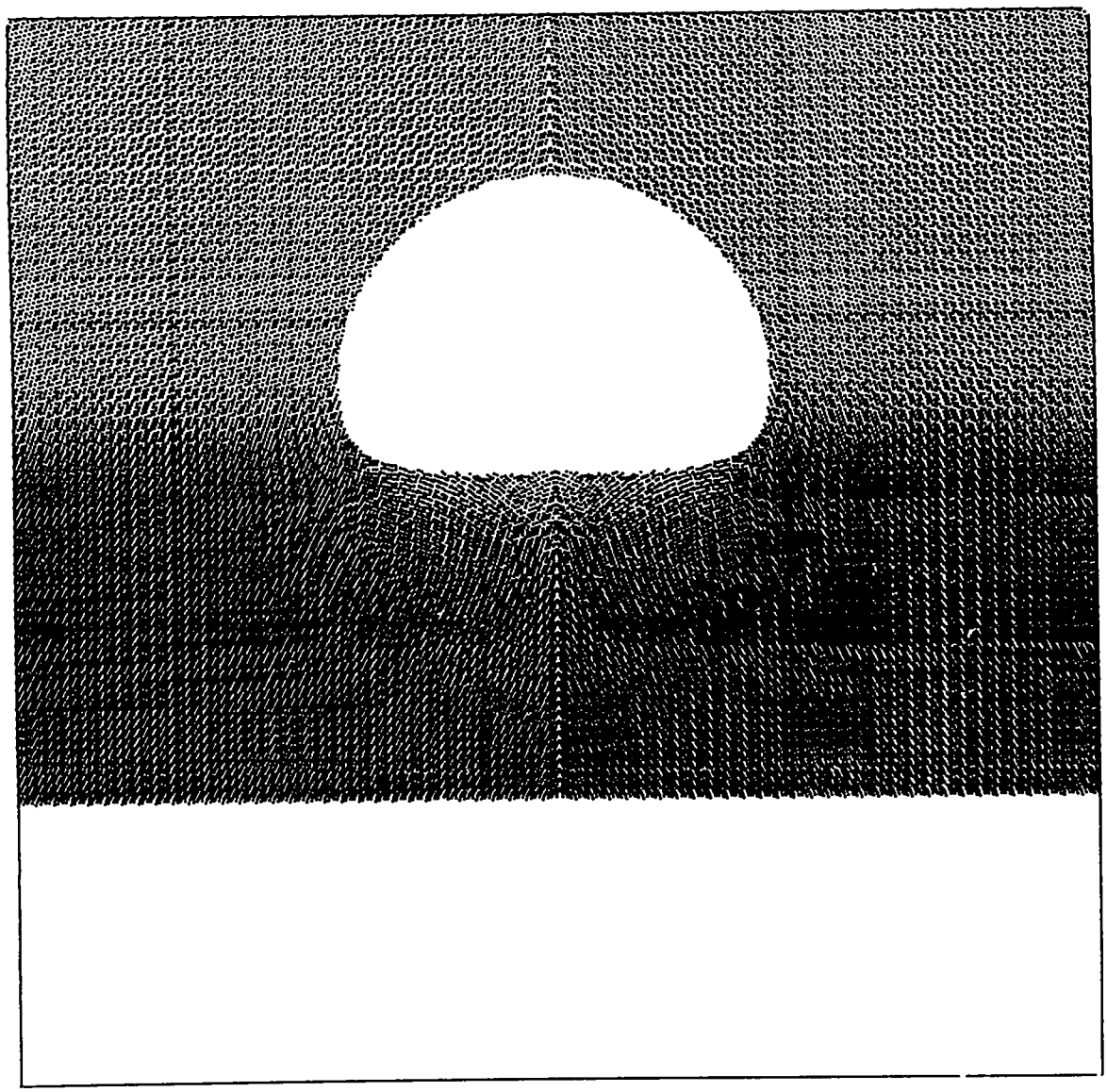

4.95 μsec

Fig. 8. The computed interaction of a shock with a 1-cm-radius cylindrical void in water centered 3.25 cm above a constant-pressure, 155-kbar piston.

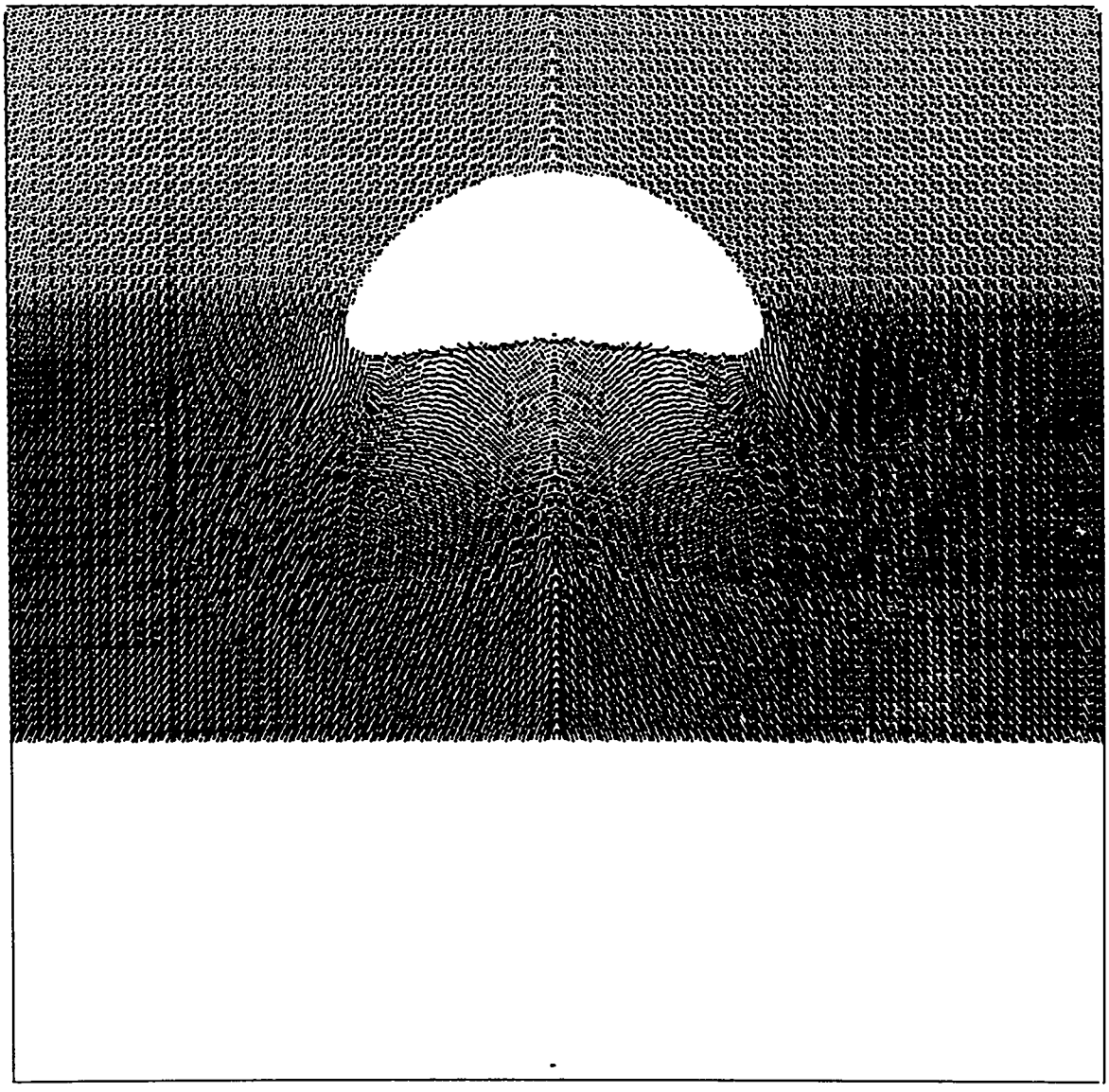

6.0 μsec

Fig. 8 (continued)

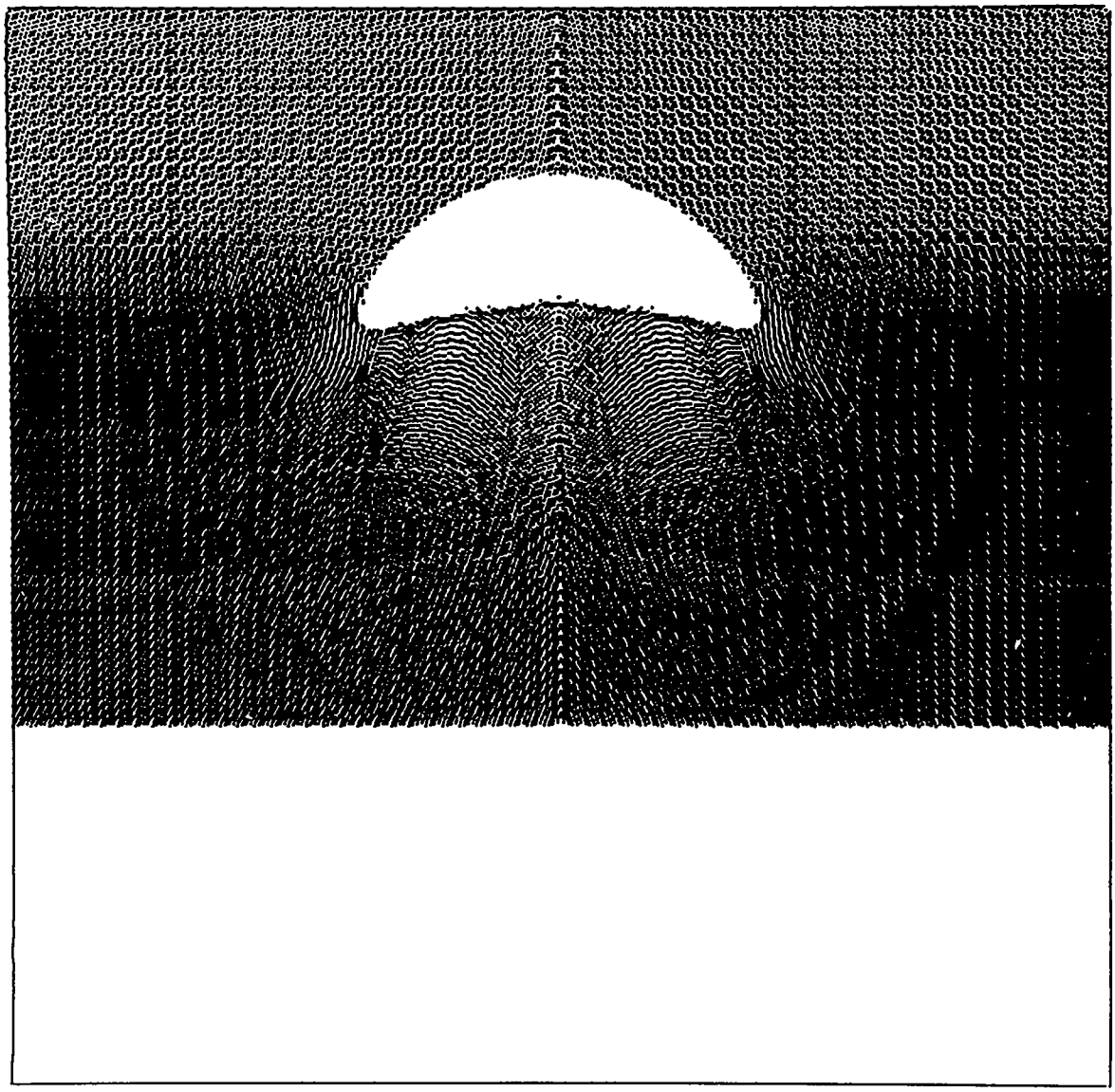

6.3 μsec

Fig. 8 (continued)

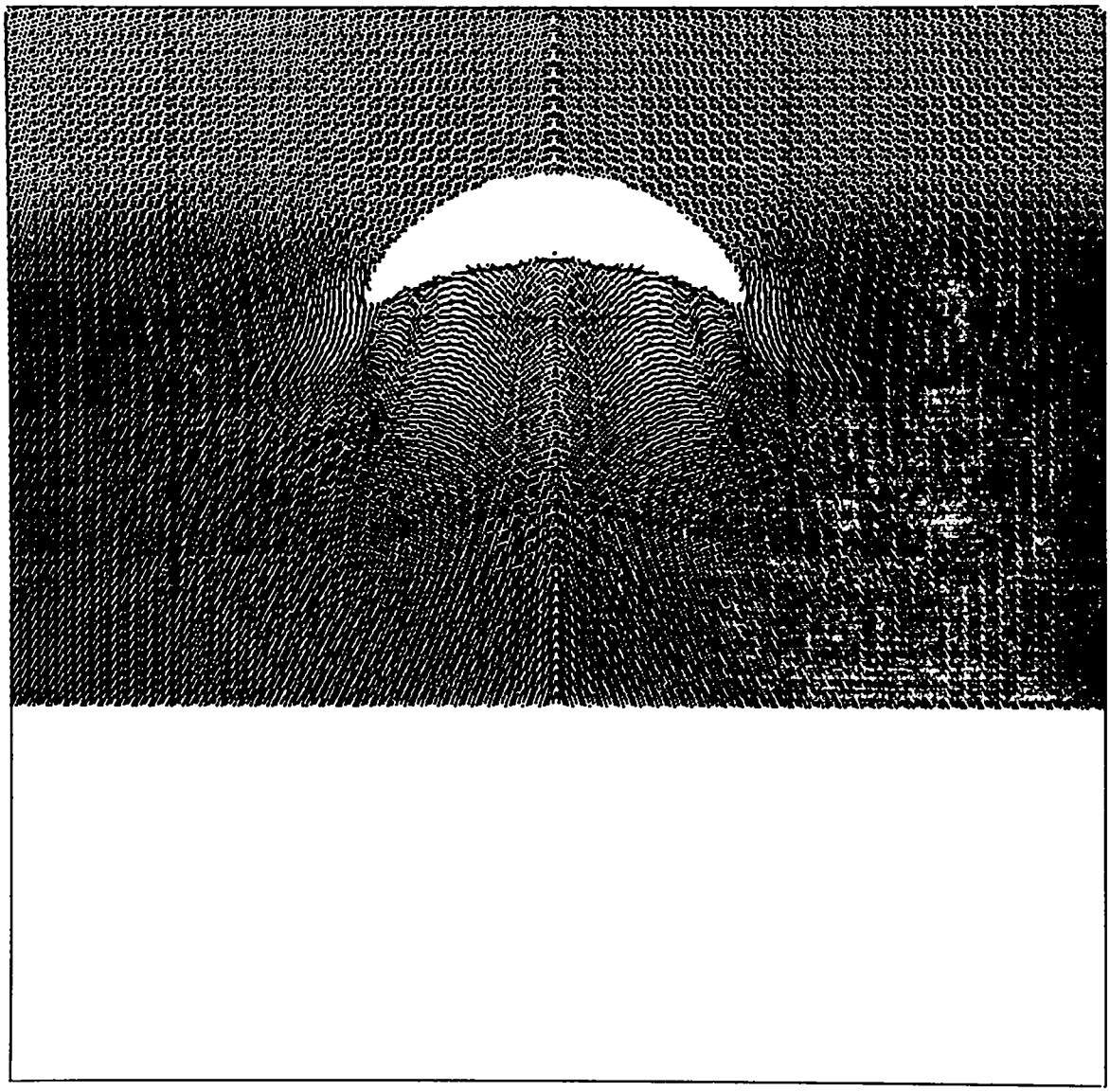

6.6 μsec

Fig. 8 (continued)

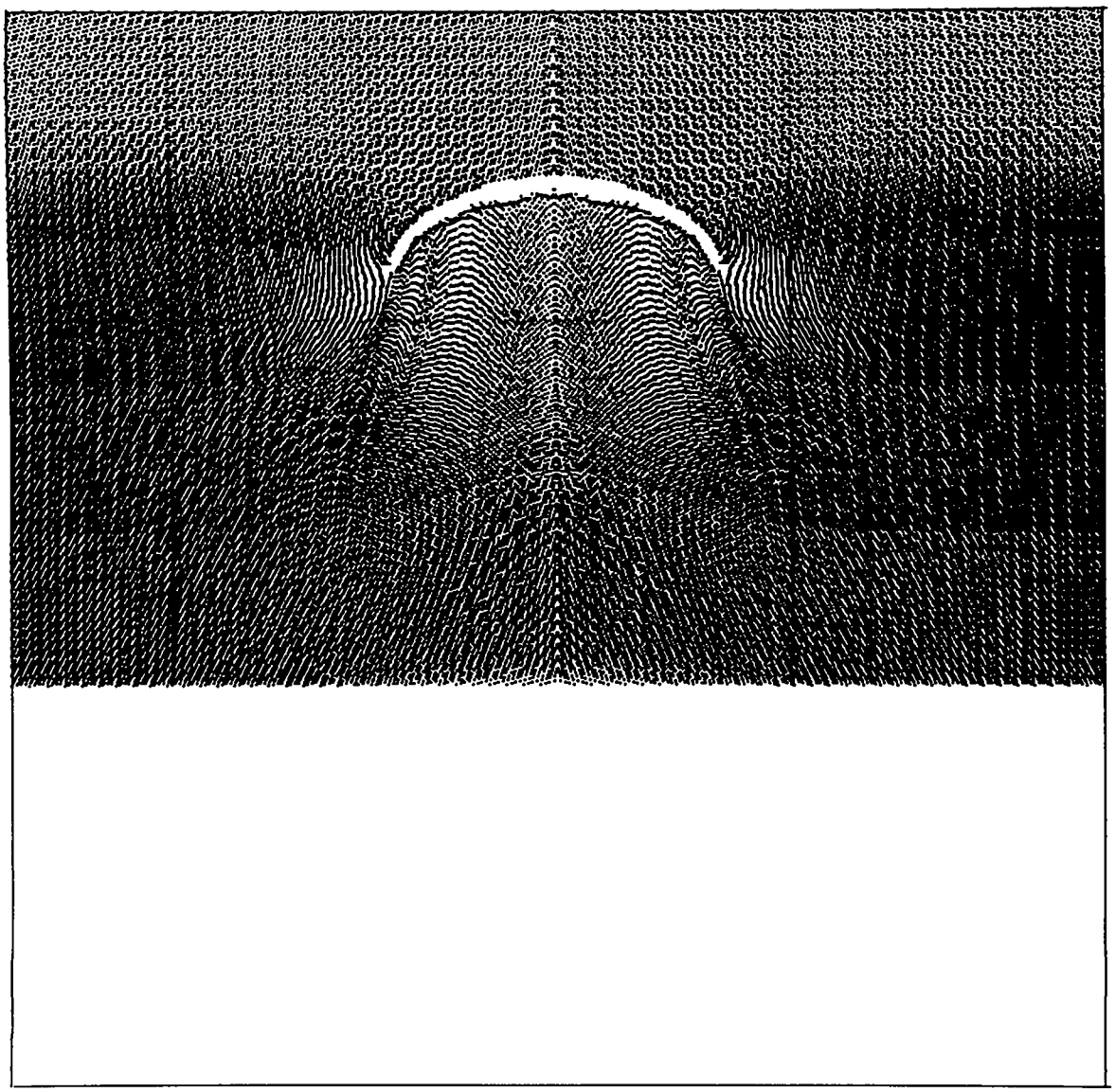

7.05 μsec

Fig. 8 (continued)

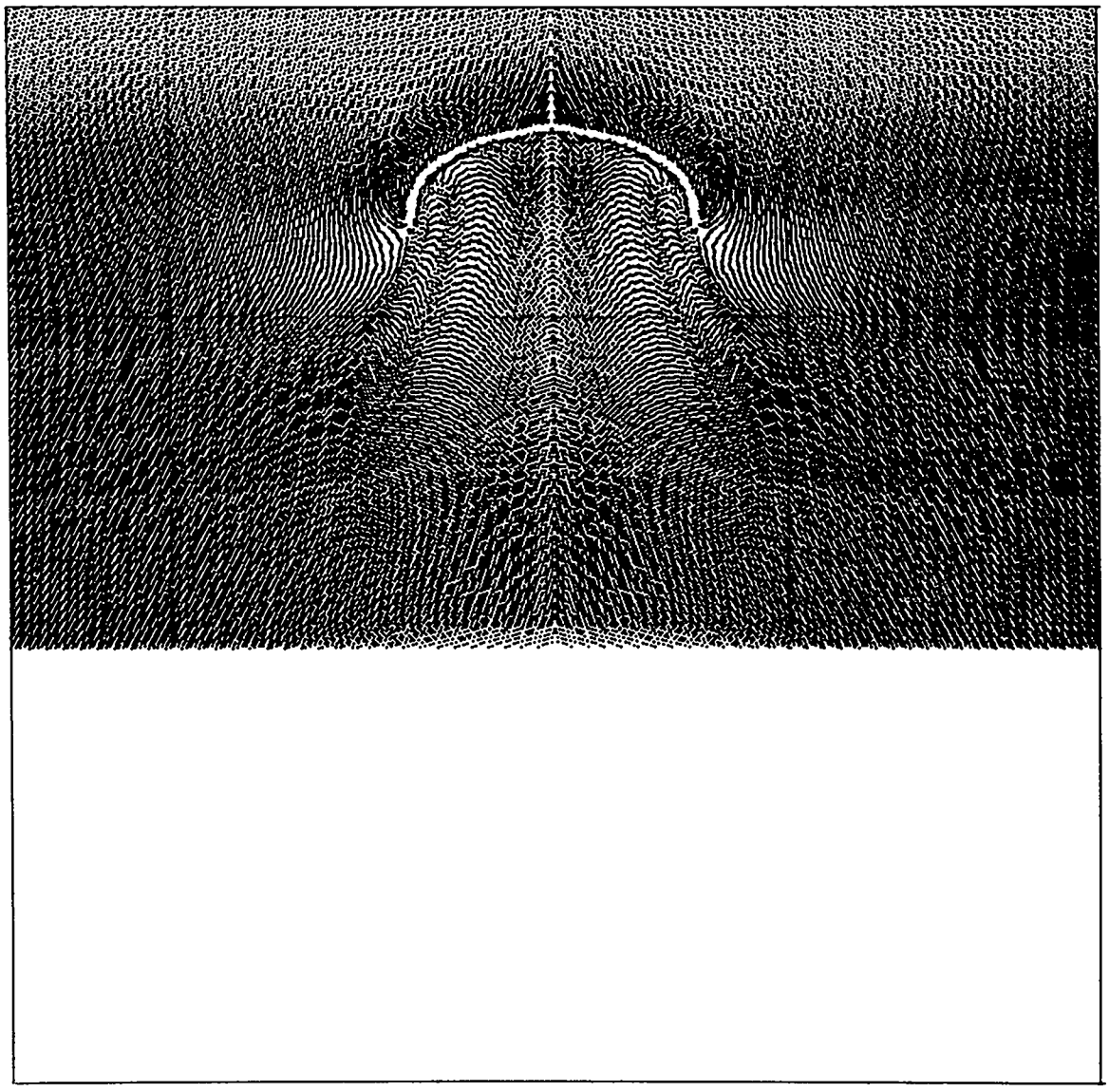

7.65 μsec

Fig. 8 (continued)

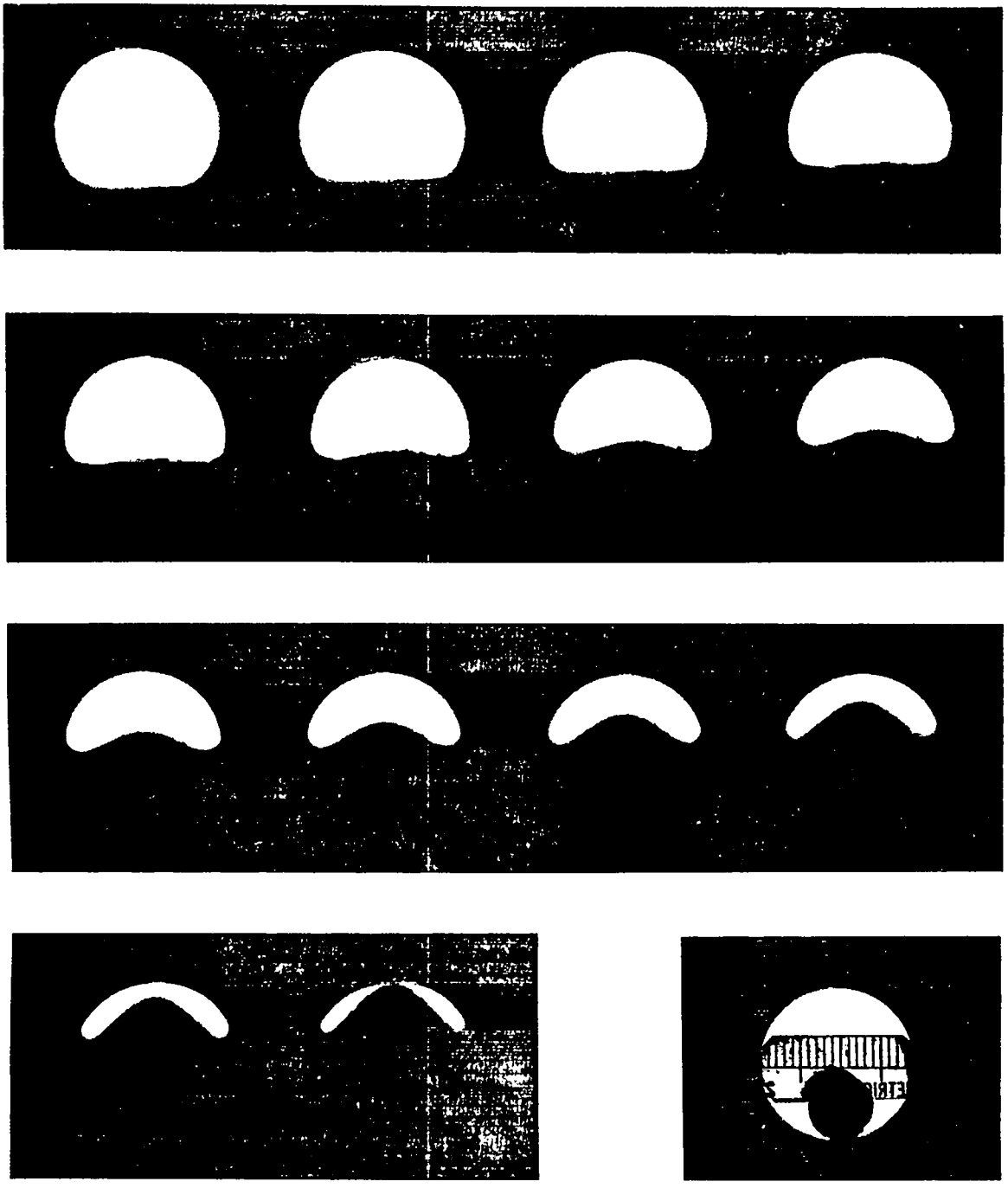

Fig. 9. Framing camera photographs of the closure of a 1-cm-radius cylindrical void in polyethylene in the same geometry as the void in water radiographs of Fig. 6. Time between frames is 0.21 μsec, and exposure time is 0.09 μsec. The last frame is a still photograph.

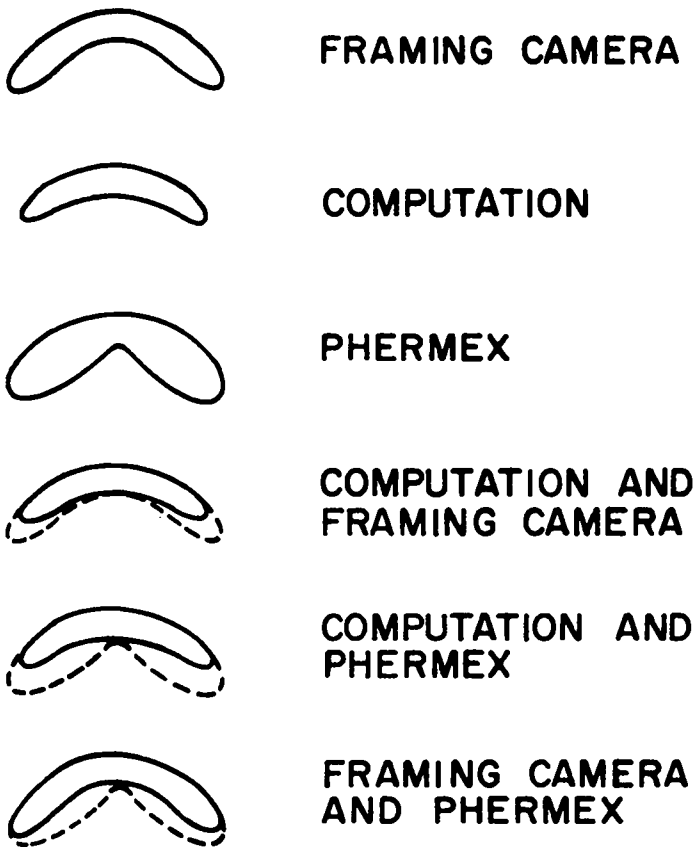

Fig. 10. The cylindrical void profile when the void is approximately 5/6 closed at the axis, as shown by computation, the framing camera, and PHERMEX.